INFN/AE-99/08-15
4 Giugno 1999

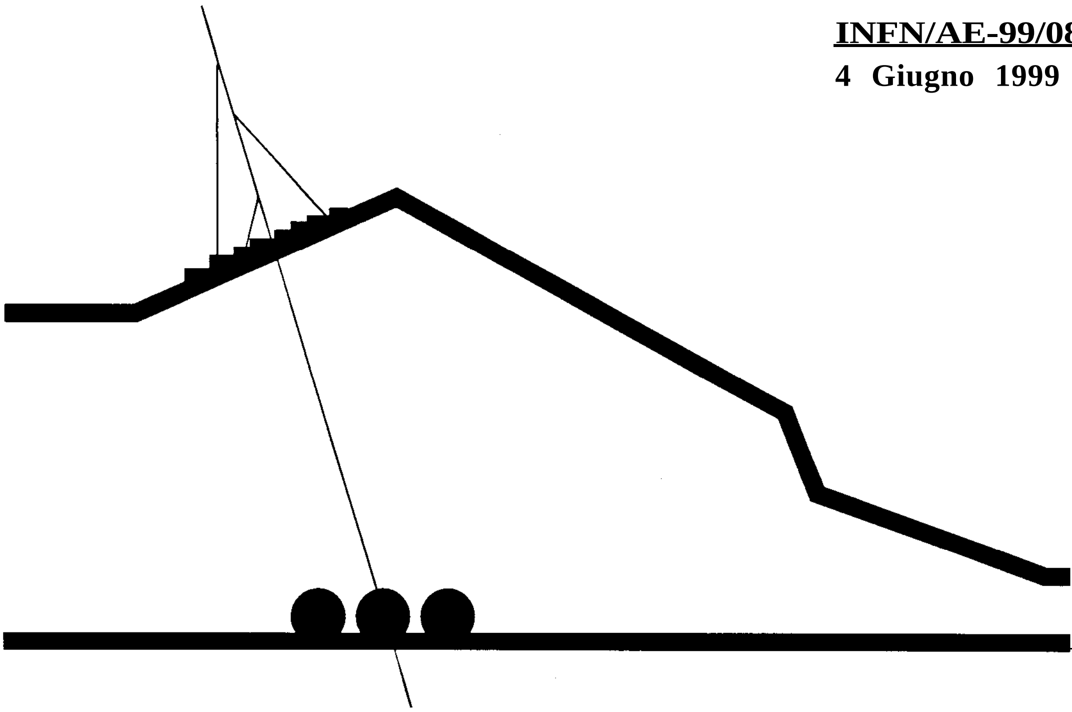

Search for Magnetic Monopoles with MACRO	INFN/AE-99/08
Neutrino Oscillation at High Energy by MACRO	INFN/AE-99/09
Low Energy Atmospheric Neutrino events in MACRO	INFN/AE-99/10
Macro as a Telescope for Neutrino Astronomy	INFN/AE-99/11
Search for WIMPS Using Upward-Going Muons in MACRO	INFN/AE-99/12
Search for Steady, Modulated and Variable Cosmic Ray Sources using Underground Muons in MACRO	INFN/AE-99/13
Moon and Sun Shadowing Observed by the MACRO Detector	INFN/AE-99/14
Transition Radiation Detector in MACRO	INFN/AE-99/15

Macro Collaboration

Contributions of the MACRO Collaboration to the 1999 Summer Conferences

INFN - Laboratori Nazionali del Gran Sasso

Published ***by*** **SIS-Pubblicazioni**
dei Laboratori Nazionali ***di Frascati***

The MACRO Collaboration

M. Ambrosia[12], R. Antolini[7], C. Aramo[7, 1], G. Auriemma[14, a], A. Baldini[13], G. C. Barbarino[12], B. C. Barish[4], G. Battistoni[6, b], R. Bellotti[1], C. Bemporad[13], E. Bernardini[7], P. Bernardini[10], H. Bilokon[6], V. Bisi[16], C. Bloise[6], C. Bower[8], M. Brigida[1], S. Bussino[18], F. Cafagna[1], M. Calicchio[1], D. Campana[12], M. Carboni[6], S. Cecchini[2, c], F. Cei[11, 13], V. Chiarella[6], B. C. Choudhary[4], S. Coutu[11, m], G. De Cataldo[1], H. Dekhissi[2, 17], C. De Marzo[1], I. De Mitri[9], J. Derkaoui[2, l7], M. De Vincenzi[18], A. Di Credico[7], O. Erriquez[1], C. Favuzzi[1], C. Forti[6], P. Fusco[1], G. Giacomelli[2], G. Giannini[13, e], N. Giglietto[1], M. Giorgini[2], M. Grassi[13], L. Gray[7], A. Grillo[7], F. Guarino[12], C. Gustavino[7], A. Habig[3], K. Hanson[11], R. Heinz[8], Y. Huang[4], E. Iarocci[6, f], E. Katsavounidis[4], I. Katsavounidis[4], E. Kearns[3], H. Kim[4], S. Kyriazopoulou[4], E. Lamanna[14], C. Lane[5], T. Lari[7], D. S. Levin[11], P. Lipari[14], N.P. Longley[4, i], M. J. Longo[11], F. Loparco[1], F. Maaroufi[2, 17], G. Mancarella[10], G. Mandrioli[2], A. Margiotta[2], A. Marini[6], D. Martello[10], A. Marzari-Chiesa[16], M. N. Mazziotta[1], D. G. Michae[14], S. Mikheyev[4, 7, g], L. Miller[8], P. Monacelli[9], T. Montaruli[1], M. Monteno[16], S. Mufson[8], J. Musser[8], D. Nicolò[13, d], C. Orth[3], G. Osteria[12], M. Ouchrifz[2, 17], O. Palamara[7], V. Patera[6, f], L. Patrizii[2], R. Pazzi[13], C. W. Peck[4], L. Perrone[10], S. Petrera[9], P. Pistilli[18], V. Popa[2, h], A. Rainò[1], A. Rastelli[7], J. Reynoldson[7], F. Ronga[6], U. Rubizzo[12], C. Satriano[14, a], L. Satta[6, f], E. Scapparone[7], K. Scholberg[3], A. Sciubba[6, f], P. Serra[2], M. Severi[14], M. Sioli[2], M. Sitta[16], P. Spinelli[1], M. Spinetti[6], M. Spurio[2], R. Steinberg[5], J.L. Stone[3], L. R. Sulak[3], A. Surdo[10], G. Tarlè[11], V. Togo[2], D. Ugolotti[2], M. Vakili[15], C. W. Walter[3] and R. Webb[15].

1. Dipartimento di Fisica dell'Università di Bari and INFN, 70126 Bari, Italy
2. Dipartimento di Fisica dell'Università di Bologna and INFN, 40126 Bologna, Italy
3. Physics Department, Boston University, Boston, MA 02215, USA
4. California Institute of Technology, Pasadena, CA 91125, USA
5. Department of Physics, Drexel University, Philadelphia, PA 19104, USA
6. Laboratori Nazionali di Frascati dell'INFN, 00044 Frascati (Roma), Italy
7. Laboratori Nazionali de1 Gran Sasso dell'INFN, 67010 Assergi (L'Aquila), Italy
8. Depts. of Physics and of Astronomy, Indiana University, Bloomington, IN 47405, USA
9. Dipartimento di Fisica dell'Università dell'Aquila and INFN, 67100 L'Aquila, Italy
10. Dipartimento di Fisica dell'Università di Lecce and INFN, 73100 Lecce, Italy
11. Department of Physics, University of Michigan, Ann Arbor, MI 48109, USA
12. Dipartimento di Fisica dell'Università di Napoli and INFN, 80125 Napoli, Italy
13. Dipartimento di Fisica dell'Università di Pisa and INFN, 56010 Pisa, Italy
14. Dipartimento di Fisica dell'Università di Roma "La Sapienza" and INFN, 00185 Roma, Italy
15. Physics Department, Texas A&M University, College Station, TX 77843, USA
16. Dipartimento di Fisica Sperimentale dell'Università di Torino and INFN, 10125 Torino, Italy
17. L.P.T.P., Faculty of Sciences, University Mohamed I, B.P. 524 Oujda, Morocco
18. Dipartimento di Fisica dell'Università di Roma Tre and INFN Sezione Roma Tre, 00185 Roma, Italy

a. Also Università della Basilicata, 85 100 Potenza, Italy
b. Also INFN Milano, 20133 Milano, Italy
c. Also Istituto TESREKNR, 40129 Bologna, Italy
d. Also Scuola Normale Superiore di Pisa, 56010 Pisa, Italy
e. Also Università di Trieste and INFN, 34100 Trieste, Italy
f. Also Dipartimento di Energetica, Università di Roma, 00185 Roma, Italy
g. Also Institute for Nuclear Research, Russian Academy of Science, 1173 12 Moscow, Russia
h. Also Institute for Space Sciences, 76900 Bucharest, Romania
i. The Colorado College, Colorado Springs, CO 80903, USA
1. Also INFN Catania, 95 129 Catania, Italy
m. Also Department of Physics, Pennsylvania State University, University Park, PA 16801, USA

INFN/AE-99/15
4 Giugno 1999

Transition Radiation Detector in MACRO

Abstract

The MACRO detector is located in the Gran Sasso Laboratory. MACRO's overburden varies from 3150 to 7000 hg/cm^2. A transition radiation detector (TRD) has been added to the MACRO detector in order to measure the residual energy of muons entering MACRO, i.e. the energy they have after passing through the Gran Sasso's rock overburden. The TRD consists of three identical modules with a total horizontal area of 36 m^2. The results presented here are referred to single and double events in MACRO with one muon crossing one of the TRD modules. Our data show that double muons are more energetic than single ones, as predicted by the interaction models of primary cosmic rays with the atmosphere.

1 Introduction:

High energy underground muons are the remnants of the air showers produced in the atmosphere by collisions of high energy cosmic ray nuclei with air nuclei. Since muons are nearly stable and have a small interaction cross section, they are called the "penetrating charged component" of cosmic rays. Thus, muons give the dominant signal deep in the atmosphere and underground. Muons carry information about the primary particle mass, the primary energy spectrum and the inelastic cross section. Underground muons also give information on energy loss in the rock.

The analysis of the energy of muons detected deep underground is one of the tools used for the indirect study of the interaction models of primary cosmic rays. As in all indirect measurements in cosmic ray physics, the final interpretation is unavoidably dependent of the model adopted to describe the secondary production and transport, and on the energy spectra and chemical composition of primaries. The energy loss of muons in the rock smears the information about primaries carried by the muons. It is therefore crucial to find physical observables which can be used to investigate the interaction models besides the energy spectra and chemical composition of the primary cosmic rays. However, it is very hard to disentangle the interaction model from spectra and composition; thus in any discussion one needs to take into account all those components, while dedicated analyses (as depth intensity, decoherence) can be used to put some constraints on the proprieties of the primary cosmic rays.

In the present paper we describe a measurement of the underground muon energy spectrum, carried out using a transition radiation detector (TRD) in association with the MACRO apparatus. In this analysis we use single and double muon events in MACRO, with one muon crossing one of the TRD modules, in order to investigate the all-particle energy spectrum of the primary cosmic rays taking into account the energy loss of the muons in the rock above the detector.

In a previous analysis (Ambrosio, et al, 1999), which can be used as reference for the detector description and for the analysis method, we used the single muons crossing the first TRD module. In the present analysis we use all the TRD modules, providing a large sample of single muons and a sufficient number of double muons.

2 Detector description:

The MACRO detector is located in Hall B of the Gran Sasso Underground Laboratory. The laboratory is located at an average depth of 3700 hg/cm^2, with a minimum depth of 3150 hg/cm^2. At these depths the residual energy differential distribution of the downgoing muons is estimated to be nearly flat up to 100 GeV and it then falls rapidly in the TeV region; the mean value is a few hundred GeV. The TRD has been designed to explore the muon energy range of 100 GeV–1 TeV. Below 100 GeV there is no transition radiation (TR) emission; from 100 GeV to 1 TeV the detector has a smoothly increasing response versus the muon energy. For energies greater than 1 TeV, where the muon flux is estimated to be approximately 5% of the total, the TR signal is saturated.

The MACRO TRD consists of three modules of 36 m^2 total horizontal area. Each module has an active volume of $6 \times 1.92 \times 1.7\ m^3$ and contains 10 planes of 32 proportional tubes, 6 meters long and with a square cross section of $6 \times 6\ cm^2$. These counters are laid close together between 11 Ethafoam radiator layers of 10 cm height to form a large multiple layer TRD with reduced inefficient zones. The ionization loss and the X-rays of TR produced by muons are detected in the proportional tubes filled with $Ar - CO_2$ mixture. A detailed description of the MACRO TRD is given in Barbarito et al., 1995.

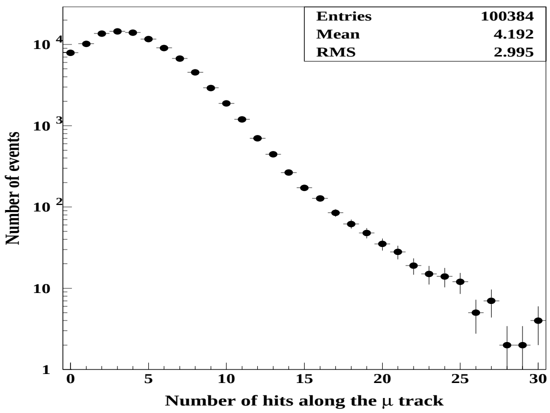

Figure 1: Hit distribution for single muon tracks crossing the first TRD module.

The first TRD module began to collect data in 1994, while the second and the third TRD modules, which were put in acquisition in 1996, are similar to the first module, but are equipped with a different front-end electronics. This is the reason why the data samples of the first and of the second and the third TRD modules need to be analyzed separately. Since the second module was built with the same structure as the third module, a joint analysis of their data is possible.

3 Data Selection:

For this analysis we have considered the data collected by the first TRD module from April 1995 to January 1999, the data collected by the second one from June 1997 to January 1999 and the data collected by the third module from January 1997 to January 1999. We have analyzed two categories of events: "single muons", i.e. single events in MACRO crossing one TRD module; and "double muons", i.e. double events in MACRO with only one muon crossing one TRD module.

Since the TRD calibration was performed for particles crossing the ten layers and at zenith angles below 45^o (Barbarito et al., 1995), in this analysis only muons fulfilling these constraints have been included. The total number of hits in the track is evaluated by counting the number of TRD hits along the straight line fitted to the track reconstructed by the MACRO detector. The total number of final events is about $2 \cdot 10^5$ for single muons and about $13 \cdot 10^3$ for double muons.

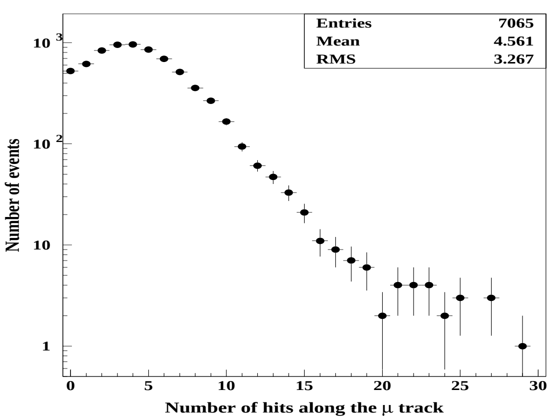

Figure 2: TRD hit distribution in the first module for double muon tracks.

In Figures 1 and 2 the distributions of the number of hits in the single muon and double muon tracks of the final event sample in the first TRD module are shown. It should be noted that the average value of the double muon distribution is greater than the one of the corresponding single muon distribution. This means that the average energy of double muons is higher than the average energy of single muons. The ratio of the difference between the average hit of double muons ($< hit >_{2\mu}$) and the average hit of single muons ($< hit >_{1\mu}$) over the average hit of single muons are $R_{hit} = (< hit >_{2\mu} - < hit >_{1\mu}) / < hit >_{1\mu} = (8 \pm 1)\%$. This ratio is correlated to the energy ratio: $R_E = (< E >_{2\mu} - < E >_{1\mu})/ < E >_{1\mu}$.

4 Muon energy spectrum:

In order to evaluate the local muon energy spectrum, we must take into account the TRD response function, which induces some distortion of the “true” muon spectrum distribution. The “true” distribution can be extracted from the measured one by an unfolding procedure that yields good results only if the response of the detector is correctly understood. We have adopted an unfolding technique, developed according to Bayes’ theorem, following the procedure described in D’Agostini, 1995 and Mazziotta, 1995.

4.1 Detector simulation The distributions of the hits collected along a muon track at fixed rock depth h by the TRD and at a given zenithal and azimuthal angle, $N(k, \vartheta, \varphi)$, can be related to the residual energy distribution of muons, $N(E, \vartheta, \varphi)$, by:

$$N(k, \vartheta, \varphi) = \sum_{j=1}^{n_E} p(k \mid E_j, \vartheta, \varphi) N(E_j, \vartheta, \varphi) \tag{1}$$

where the detector response function, $p(k \mid E_j, \vartheta, \varphi)$, represents the probability to observe k hits for a track of a given energy E_j and at a given angle ϑ and φ. The response function must contain both the detector acceptance and the event reconstruction efficiency. We have derived the response function by simulating the MACRO behaviour using GEANT (Brun et al., 1992), including the trigger efficiency simulation. The simulation of the TRD was based on the test beam calibration data, taking into account the inefficiency of the proportional tubes. A check of the response function of the TRD is obtained by using low energy muons, namely stopping muons and muons with large scattering angles in MACRO, which have energies of about $1 - 2\ GeV$ (Ambrosio et al, 1999).

4.2 Experimental data distributions The unfolding procedure has been applied separately to the TRD data samples of the first module, and of the second and the third modules, starting with a trial spectrum assigned to the unfolded distribution (D’ Agostini, 1995; Mazziotta, 1995), according to a local energy spectrum of muons at 4000 hg/cm^2 with a spectral index fixed at 3.7 given by (Lipari and Stanev, 1991):

$$N_o(E, h) \sim (E + \epsilon(1 - e^{-\beta h}))^{-\alpha} \tag{2}$$

The parameters are: $h = 4000\ hg/cm^2$, $\alpha = 3.7$, $\beta = 0.383\ 10^{-3}\ cm^2/hg$, $\epsilon = 618\ GeV$ and $E(GeV)$.

The TRD response is saturated for $E_\mu \geq 1\ TeV$; for energies larger than $1\ TeV$ only the number of events

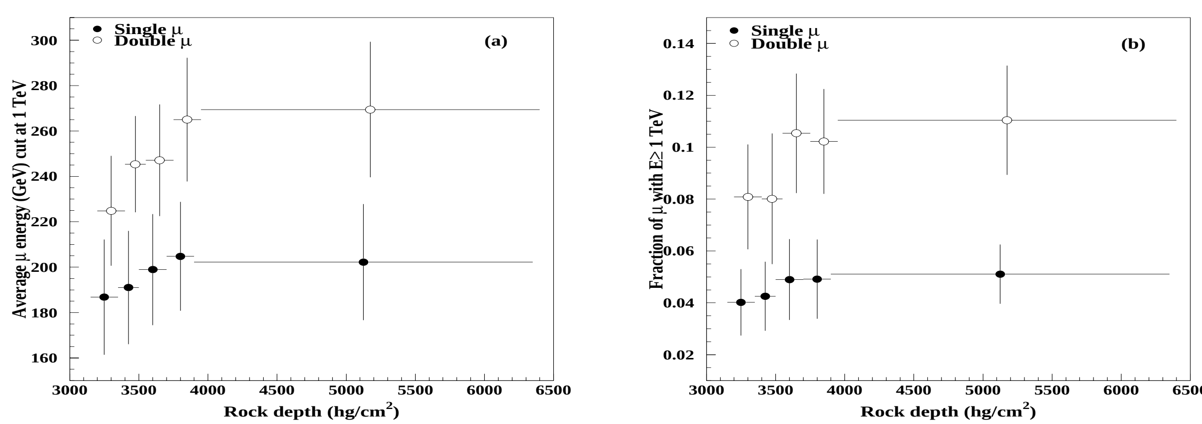

Figure 3: (a) Average muon energy computed with a cut at $1\ TeV$; (b) fraction of muons with energies greater than $1\ TeV$ versus the standard rock depth.

can be evaluated, while below $1\ TeV$ we can reconstruct the energy distribution and we can compute the average value cut to $1\,TeV$.

In Fig. 3a the average energies of single muons (black circles) and of double muons (open circles) for muons with $E_\mu < 1\,TeV$ are plotted versus the standard rock depth. Fig. 3b shows the fraction of events with energy greater than $1\,TeV$ versus the standard rock depth. The values quoted in these figures have been obtained by combining the results coming from the three TRD modules. The error bars include statistical and estimated systematic uncertainties.

The average muon energy for single muons with $E_\mu < 1\,TeV$ is $196{\pm}3\,(stat){\pm}25\,(syst)\,GeV$; for double muons it is $247 \pm 13\,(stat) \pm 25\,(syst)\,GeV$. The fraction of single muon events with energies greater than $1\,TeV$ is $4.6{\pm}0.1\,(stat){\pm}1.4\,(syst)\,\%$, while for the double muon events it is $9.4{\pm}0.6\,(stat){\pm}1.4\,(syst)\,\%$.

The experimental average muon energy over all energies was calculated by adding to the average energy obtained with an energy cut at $1\,TeV$ the contribution from muons of greater energy. The high energy contribution was estimated by multiplying the measured fraction of muons with energy $\geq 1\,TeV$ by the average muon energy above $1\,TeV$:

$$<E_\mu> = (1 - f) \cdot <E_\mu>_{cut} + f \cdot <E_\mu>_{nocut} \quad (3)$$

where f is the fraction of events with $E \geq 1\,TeV$ (measured), $<E>_{cut}$ is the average energy with $E < 1\,TeV$ (measured) and $<E>_{nocut}$ is the average energy with $E \geq 1\,TeV$ (calculated).

The evaluation of $<E>_{nocut}$ was based on a simple extrapolation of the local energy spectrum as reported in Equation (2) using the same parameters for the depth interval shown in Fig. 3. The average single muon energy obtained in this way is $272 \pm 4\,(stat) \pm 33\,(syst)\,GeV$, while for the double muons it is $398 \pm 16\,(stat) \pm 39\,(syst)\,GeV$.

These values of average muon energies do not change appreciably with variations of β, ϵ, and α. Varying each of these three parameters by 3%, which is a value typically quoted (Battistoni 1997), results in a change in the average energies of 0.1%, 0.2%, and 1% respectively. These uncertainties are significantly smaller than our quoted error.

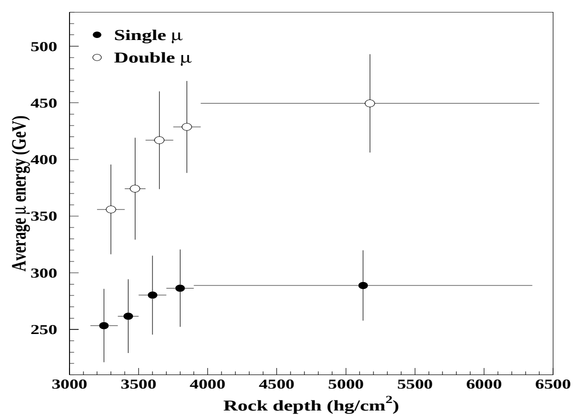

Figure 4: Average muon energy versus the standard rock depth.

Fig. 4 shows the average for single muon energies (black circles) and for double muons (open circles) as a function of rock depth. The double muons are more energetic than single ones, as predicted by the interaction models of primary cosmic rays with the atmosphere.

References

Ambrosio, M., Antolini, R., Aramo, C., et al., 1999, Astroparticle Physics 10, 11

Barbarito, E., Bellotti, R., Cafagna, F. et al., 1995, Nucl. Instr. Meth. A 365, 214

D'Agostini, G., Nucl. Instr. Meth., 1995, A 362, 487

Mazziotta, M. N., 1995, LNGS 95/52

Brun, R. et al., 1992, CERN Public. DD/EE/84-1

Lipari, P. and Stanev, T., 1991, Phys. Rev. D 44, 3543

Battistoni, G., Ferrari, A., Forti, C. and Scapparone, E., 1997, Nucl. Instr. Meth., A 394, 136